KSABC
The Korean Society for Applied Biological Chemistry

ARTICLE

Open Access

Metabolomics reveals that *Curcuma longa* and demethoxycurcumin inhibit HCT116 human colon cancer cell growth

Dahye Yoon[1], Bo-Ram Choi[1], Woo Cheol Shin[1], Kwan-Woo Kim[1], Young-Seob Lee[1] and Dae Young Lee[1*]

Abstract

Studies on the use of natural products to treat cancer are ongoing, and turmeric (*Curcuma longa* L.), a medicinal crop, is known for various effects including anticancer activity. In this study, the inhibitory effect of *C. longa* and demethoxy-curcumin on cancer cell growth in a colorectal cancer cell line (HCT116) was investigated by using nuclear magnetic resonance (NMR) spectroscopy-based metabolomics. For this analysis, HCT116 cells were treated with doxorubicin (positive control), *C. longa* extract, or demethoxycurcumin (20, 40, and 60 μM). In the NMR spectra of the HCT116 cell extract, 45 metabolites were identified and quantified. The quantified metabolites were analyzed by biomarker analysis, and significantly changed metabolites were filtered by the area under the curve (AUC) of the receiver operator characteristic (ROC) curve. Multivariate statistical analysis of NMR spectra was conducted to confirm the distribution among groups. Through an S-line plot, it was possible to identify metabolites that contributed to the differences seen in the OPLS-DA score plot. Taken together, the results reveal that *C. longa* extract induces oxidative stress and changes the energy metabolism in HCT116 cells, and that demethoxycurcumin inhibits the energy metabolism strategy for the survival of cancer cells, escape from immune cells, and cancer cell proliferation, thereby enabling the survival of HCT116 cells.

Keywords Colon cancer, Metabolomics, *Curcuma longa*, Demethoxycurcumin

Introduction

While medical technology to extend human lifespan continues to develop, cancer mortality is still high, and the social burden is also increasing [1]. In particular, colorectal cancer has a high diagnosis rate, and although it has a high survival rate in the early stage, its mortality rate is high among all cancers [2]. When colorectal cancer is detected early, the cure rate is high, but it is often detected late because certain symptoms or pain do not appear in the early stages. With continuing research on conquering cancer, first-generation chemical anticancer drugs, second-generation targeted anticancer drugs, and third-generation immune anticancer drugs have been developed, and recently, fourth-generation anticancer drugs are being developed. Existing anticancer drugs have disadvantages such as side effects and resistance. Natural products are compounds produced by living organisms in nature that can be used as food, and it is expected that safe natural products can be used for anticancer therapy to compensate for the shortcomings of existing anticancer drugs.

Turmeric (*Curcuma longa* L.) is a perennial herbaceous plant belonging to the Zingiberaceae family that is cultivated in India, Indonesia, China, and other Asian countries. *C. longa* is frequently used as a medicinal herb and a food supplement owing to its health benefits. *C. longa* is known for many biological activities, among which anticancer activity has been reported, including against

*Correspondence:
Dae Young Lee
dylee0809@gmail.com
[1] Department of Herbal Crop Research, National Institute of Horticultural and Herbal Science, RDA, Eumseong, Chungbuk 27709, Republic of Korea

Yoon *et al. Applied Biological Chemistry*   (2023) 66:84

Page 2 of 10

glioma cancer [3], cervical cancer [3], prostate cancer [3, 4], oral cancer [4], breast cancer [5, 6], colon cancer [7], and liver cancer [8] in vitro, and liver cancer [9], colon cancer [10], and breast cancer [11] in vivo.

In addition to studies on extracts, many anticancer studies have been conducted on major compounds contained in *C. longa*. As a representative compound of *C. longa*, curcumin has been reported to be highly cytotoxic to cancer cells. DNA damage [12], c-jun N-terminal kinase dependent apoptosis [13], and downregulation of E2F4 expression and apoptosis [14] were investigated in the human colon cancer cell line (HCT116) treated with curcumin. Curcumin is easily converted to demethoxycurcumin by demethoxylation from its benzene ring, resulting in a more stable structure [15]. Demethoxycurcumin has also been subjected to cytotoxic studies of cancer cell lines including fibrosarcoma [16], breast cancer [17], prostate cancer [18], lung cancer [19–21], bladder cancer [22], cervical cancer [23], oral squamous cell carcinoma [24], osteosarcoma [25], and brain glioblastoma [26]. However, there are no reports on colorectal cancer. We tried to confirm the growth-inhibiting activity of *C. longa* extract in colorectal cancer cells, as well as whether demethoxycurcumin exhibited the same activity. To support the interpretation of their metabolic mechanisms, metabolites of colorectal cancer cells treated with extract of *C. longa* and demethoxycurcumin were analyzed using nuclear magnetic resonance (NMR) spectroscopy. Metabolites are final products generated by metabolic processes, and because they reflect reactions that occur in the body, insight into the mechanism of cancer cells can be additionally obtained by applying metabolomics.

Materials and methods
Plant materials
The *Curcuma longa* used in this study was cultivated in the Jindo region of the Republic of Korea. A voucher specimen (MPS004295) was deposited at the Herbarium of the Department of Herbal Crop Research, National Institute of Horticultural and Herbal Science, Rural Development Administration, Eumseong, Republic of Korea. Dried rhizome of *C. longa* was ground and extracted twice by reflux extraction with 50% aqueous fermented ethanol at 80 °C for 4 h. The extract was filtered through a filter paper (Whatman, Maidstone, UK) and vacuum-concentrated under reduced pressure. The concentrated extract was lyophilized under reduced pressure (100 mTorr) (EYELA, Tokyo, Japan). Demethoxycurcumin was isolated from the *C. longa* using medium-pressure liquid chromatography (MPLC), NMR techniques and comparison with literature sample (Sigma, CAS # 22608-11-3).

Cell culture
The HCT116 human colorectal cancer cell line was purchased from the Korean Cell Line Bank (Seoul, Korea). HCT116 cells were cultured in DMEM containing 10% FBS with 100 U/mL penicillin and 100 U/mL streptomycin, and cultured at 37 °C in an atmosphere containing 5% CO_2.

Cell viability assay
HCT116 cells (2×10^4 cells/well) were seeded in 96-well plates, and cell viability was detected using 3-(4,5-dimethylthiazol-2-yl)-2,5-diphenyltetrazolium bromide (MTT). HCT116 cells were cultured with various concentrations of *C. longa* extract (0, 50, 100, 200, and 300 μg/mL) or demethoxycurcumin (0, 1.5, 3.125, 6.25, 12.5, 25, and 50 μM). Following treatment for 24 h, 10 μL MTT solution (0.5 mg/mL) was added to each well, and cells were incubated at 37 °C for 2 h. The culture medium was subsequently removed and 100 μL dimethyl sulfoxide was added to each well at room temperature while being shaken for 20 min. The optical density of HCT116 cells was measured at 570 nm wavelength on a multiwell plate reader.

Western blot analysis
HCT116 cells (5×10^5 cells/well) were seeded in 6-well plates, and the expression of PARP, caspase-3, caspase-9, Bcl-2, Bax, and p53 protein was detected via Western blot analysis. Following treatment for 24 h with demethoxycurcumin (0, 20, 40, and 60 μM) or doxorubicin (1 μM), HCT116 cells were washed twice with ice-cold PBS and lysed for 30 min on ice in cell-lysis buffer (1×RIPA; Thermo Fisher Scientific, USA). Protein concentration was determined using a BCA protein assay kit. Protein samples (10–30 μg/well) were resolved using 10% SDS-PAGE. Separated proteins were subsequently transferred onto polyvinylidene difluoride (PVDF) membranes at 70 V for 1.5 h. The membranes were blocked with 5% nonfat milk powder in TBS Tween 20 (TBST) buffer at room temperature for 1 h with shaking. The PVDF was incubated with anti-PARP (1:1000; Cell Signaling Technology, USA), anti-cleaved caspase-3 (1:1000; Cell Signaling Technology, USA), anti-cleaved caspase-9 (1:1000; Cell Signaling Technology, USA), anti-Bcl-2 (1:500; Santa Cruz Biotechnology, USA), anti-Bax (1:500, Santa Cruz Biotechnology, USA), anti-p53 (1:1000, Santa Cruz Biotechnology, USA) and anti-β-actin (1:5000, Santa Cruz Biotechnology, USA) at room temperature for 3 h. Following 3 washes with TBST twice for 30 min, the membranes were incubated with anti-immunoglobulin secondary antibody (1:2000–1:5000, Santa Cruz Biotechnology, USA) at room temperature for 1 h with shaking.

Yoon *et al. Applied Biological Chemistry*   (2023) 66:84

Page 3 of 10

The bands were detected using an Enhanced Chemiluminescence Prime Western blotting kit (Thermo Fisher Scientific, USA). Statistical significance was tested using Student's *t*-test. $P < 0.05$ was considered statistically significant.

Sample preparation for NMR analysis

For the metabolic analysis, HCT116 cells were cultivated in the same conditions as the cell viability assay. In order to obtain statistical significance, 10 samples of the control group (CON), 11 samples of the doxorubicin-treated group (DOX), and 10 samples of the *C. longa*-treated group (CL) were cultivated and analyzed. In addition, 10 samples of CON, 11 samples of DOX, 10 samples of the demethoxycurcumin 20 µM group, 10 samples of the demethoxycurcumin 40 µM group, and 10 samples of the demethoxycurcumin 60 µM group were cultivated and analyzed. Harvested HCT116 cells were washed 3 times with PBS, then an HCT116 cell pellet (approximately 1×10^7 cells) was suspended in 400 µL of pre-chilled methanol, and 325 µL of cold water and 400 µL of cold chloroform were added step-by-step. After centrifugation (4 °C, 4000 rpm, 10 min), aqueous phase and organic phase were separated. The aqueous phase of each sample was collected in a glass vial and the methanol in the sample was eliminated using SpeedVac (EYELA, Tokyo, Japan) for 6 h, and all solvent was lyophilized overnight. Samples were re-dissolved using 560 µL of deuterated 0.2 M sodium phosphate buffer containing 0.2 mM of 3-(trimethylsilyl) propionic-2,2,3,3-d_4 acid sodium salt (TSP-d_4) and transferred to 5 mm NMR tubes.

NMR data acquisition and processing

One-dimensional (1D) ^{1}H-NMR spectroscopy was conducted using a 700 MHz Bruker NMR spectrometer (Bruker Biospin, Germany) equipped with a cryoprobe at the KBSI Ochang Center, Republic of Korea. Pulse sequence for 1D experiment was a ^{1}H nuclear Overhauser effect spectroscopy (NOESY). The parameters were set as 2.00 s of relaxation delay, 50.0 ms of mixing time, 12.2 µs of 90º pulse width, and 128 transients. This resulted in a total experiment time of 7 min 48 s. Two-dimensional (2D) NMR spectroscopy experiments were performed using a 900 MHz Bruker NMR spectrometer equipped with a cryoprobe at the KBSI Ochang Center. 2D ^{1}H-^{1}H correlation spectroscopy (COSY) and ^{1}H-^{13}C heteronuclear single quantum correlation (HSQC) were performed. All acquired data were manually phased and baseline corrected using Topspin v3.6.5 (Bruker Biospin, Germany). Metabolic identification and quantification were performed using Chenomx NMR Suite 8.4 Professional (Chenomx Inc., Edmonton, Canada). Biomarker and correlation analyses of quantified metabolites were conducted by MetaboAnalyst 5.0 (https://www.metaboanalyst.ca). For multivariate statistical analysis, NMR spectra were binned to 0.001 ppm size and normalized to total area using Chenomx NMR Suite 8.4 Professional. The binning results were aligned by the icoshift algorithm of MATLAB (MathWorks, USA). Principal component analysis (PCA) and orthogonal partial least square discriminant analysis (OPLS-DA) were performed using SIMCA 15.0.2 (Umetrics, Sweden).

Results and discussion

The cytotoxic effects of *C. longa* extract and demethoxycurcumin, a single compound in the plant, on the HCT116 cell line were examined by MTT assay. The results show that HCT116 cell growth was dose-dependently inhibited by *C. longa* extract treatment for 24 h (Fig. 1A) and 48 h (Fig. 1B). The cell viability was less than 40% after treatment with 300 µg/mL of *C. longa* extract for 24 h, and less than 20% after treatment with 300 µg/
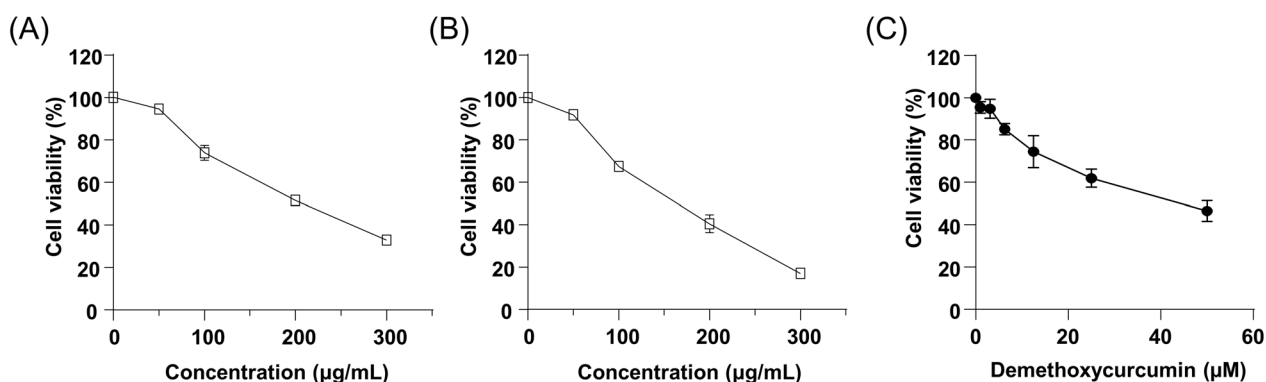

Fig. 1 Effects of *C. longa* extract or demethoxycurcumin on cell viability of HCT116 cells. **A** Cell viability of HCT116 cells treated with *C. longa* extract (0, 50, 100, 200, and 300 µg/mL) for 24 h and **B** 48 h, **C** Cell viability of HCT116 cells treated with demethoxycurcumin (0, 1.5, 3.125, 6.25, 12.5, 25, and 50 µM) for 24 h

mL of extract for 48 h. *C. longa* extract effectively inhibited the survival of HCT116 cells. Demethoxycurcumin treatment also inhibited the growth of HCT116 cells in a dose-dependent manner (Fig. 1C). *C. longa* extract majorly contains curcumin, and there have been many reports of curcumin inhibiting the growth of HCT116 cells [12–14]. As a result of confirming the cytotoxicity of the single compound contained in *C. longa*, the IC_{50} of curcumin was 12 µM (data was not shown), and the IC_{50} of demethoxycurcumin was 38.5 µM. The reason why *C. longa* extract effectively inhibited the growth of the HCT116 cell line is expected to be due to the combined action of the activity of curcumin, which is high in turmeric extract, and the activity of demethoxycurcumin. We attempted to determine how *C. longa* extract and demethoxycurcumin affect metabolic changes associated with HCT116 cell growth inhibition.

To confirm the metabolic perturbation by *C. longa* treatment in HCT116 cells, NMR-based metabolic analyses were performed. To obtain the 1D ^{1}H-NMR spectra, a 700 MHz NMR spectrometer was used. To identify metabolites in the 1D spectra, 2D COSY and HSQC-DEPT experiments were performed using a 900 MHz NMR spectrometer. All spectra were analyzed for identification and quantification of metabolites using Chenomx NMR suite software, the open Human Metabolome Database (HMDB), and measured 2D NMR spectra (Additional file 1: Figures S1 and S2). A total of 45 primary metabolites were analyzed in the extract of HCT116 cells (Additional file 1: Table S1). Figure 2 shows a representative NMR spectrum of the HCT116 extract and annotation of identified metabolites.

Quantified metabolites were analyzed by biomarker discovery analysis using receiver operator characteristic (ROC) curves with sensitivity and specificity. The area under the ROC curve (AUC) for each metabolite was calculated when comparing the *C. longa* extract treated group with the control group and the
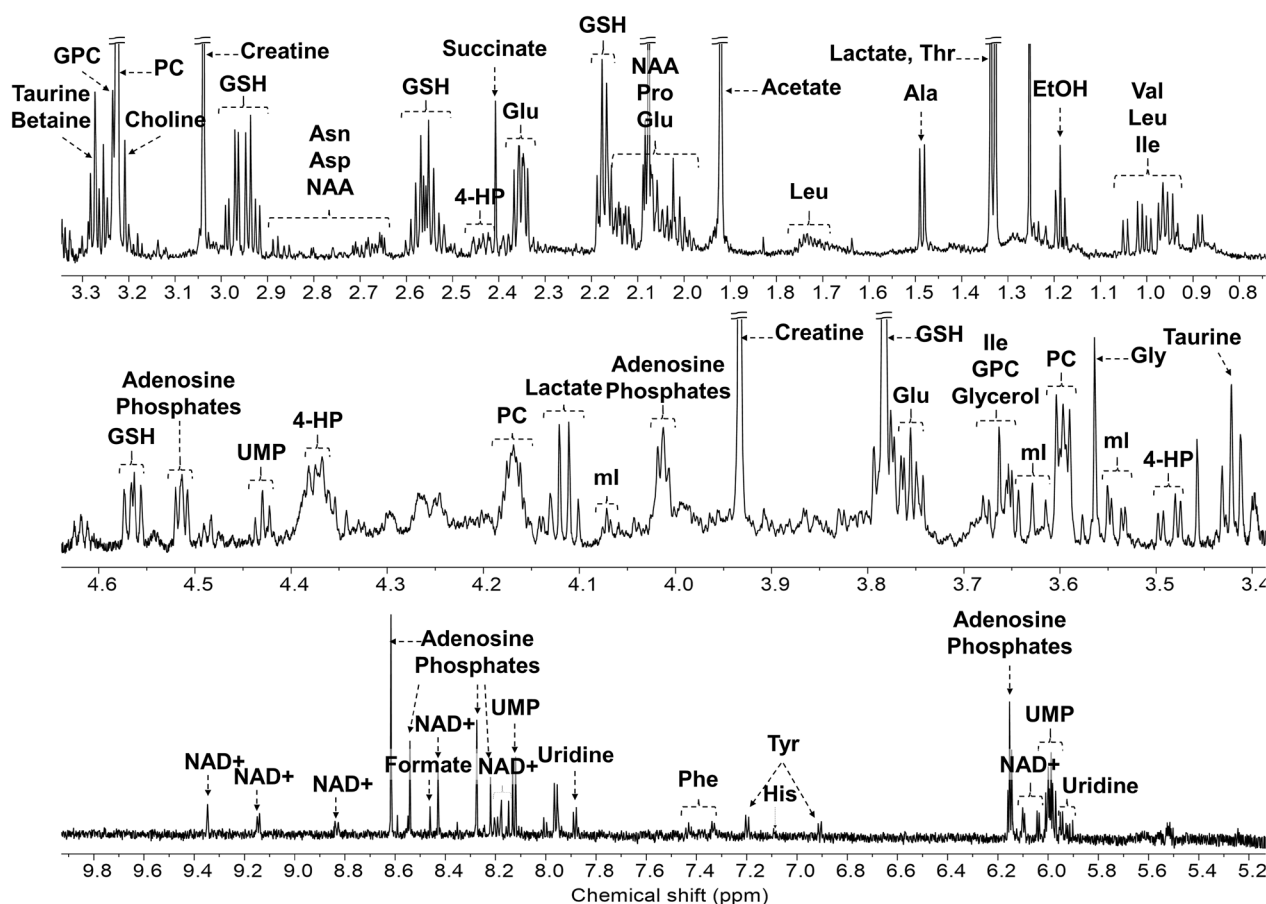

Fig. 2 Representative one-dimensional NMR spectra of the HCT116 cell extract with annotation of major metabolites. *4-HP trans*-4-hydroxy-L-proline, *Ala* alanine, *Asn* asparagine, *Asp* aspartate, *Glu* glutamate, *Gly* glycine, *GPC sn*-glycero-3-phosphocholine, *GSH* glutathione, *His* histidine, *Ile* isoleucine, *Leu* leucine, *mI myo*-inositol, *NAA N*-acetylaspartate, *PC O*-phosphocholine, *Phe* phenylalanine, *Pro* proline, *Thr* threonine, *Tyr* tyrosine, *Val* valine

Yoon *et al. Applied Biological Chemistry*   (2023) 66:84

Page 5 of 10

Table 1 Potential biomarkers of metabolites for filtering significantly changed by *C. longa* extract and demethoxycurcumin 60 μM treatment (AUC ≥ 0.7)

CON → CL			CON → DMC60		
Metabolites	**AUC**	**Concentration changes**	**Meta-bolites**	**AUC**	**Concen-|tration changes**
Alanine[***]	1.00	↑	AMP[***]	1.00	↓
Arginine[***]	1.00	↑	Formate[***]	1.00	↓
Aspartate[***]	1.00	↓	Glycine[***]	1.00	↑
Betaine[***]	1.00	↓	Lactate[***]	1.00	↑
Creatine[***]	1.00	↓	NAD+[***]	1.00	↓
Glutamate[***]	1.00	↓	Succinate[***]	1.00	↑
GSH[***]	1.00	↑	UDP-NAG[***]	1.00	↓
Glycine[***]	1.00	↓	UMP[***]	1.00	↓
Lactate[***]	1.00	↑	Uracil[***]	1.00	↑
Phenylalanine[***]	1.00	↓	Uridine[***]	1.00	↓
Threonine[***]	1.00	↓	mI[***]	1.00	↓
Uracil[***]	1.00	↑	GPC[***]	1.00	↓
Valine[***]	1.00	↓	Aspartate[***]	0.99	↓
Methionine[***]	0.99	↓	Valine[***]	0.97	↑
Serine[***]	0.99	↓	ADP[***]	0.94	↓
Taurine[***]	0.99	↓	4HP[**]	0.94	↓
DMA[**]	0.95	↓	DMA[**]	0.91	↓
Isoleucine[***]	0.95	↓	Inosine[***]	0.91	↓
Leucine[***]	0.95	↓	Glycerol[**]	0.90	↑
Histidine[**]	0.92	↓	Tyrosine[***]	0.90	↑
Tyrosine[***]	0.92	↓	NAA[**]	0.89	↓
Uridine[***]	0.85	↓	ATP[**]	0.86	↓
Succinate[**]	0.83	↓	Acetate[**]	0.84	↓
mI[*]	0.82	↓	Leucine[*]	0.83	↑
NAA[*]	0.81	↑	Betaine	0.83	↓
GPC[*]	0.80	↓	Threonine[*]	0.80	↑
NAD+[*]	0.78	↑	Choline[*]	0.77	↓
Formate[*]	0.73	↓	Glucose	0.77	↓
ATP	0.70	↓	Histidine[*]	0.76	↑
			Isoleucine	0.73	↑
			Glutamate	0.71	↑
			PC[*]	0.71	↓

[*], statistically different from control group with $p < 0.05$; [**], statistically different from CON with $p < 0.01$; [***], statistically different from CON with $p < 0.001$. *DMA* dimethylamine, *mI* myo-inositol, *4-HP trans*-4-hydroxy-L-proline, *GSH* glutathione, *PC O*-phosphocholine, *NAA N*-acetylaspartate, *GPC sn*-glycerol-3-phosphocholine, *UDP-NAG* UDP-*N*-acetylglucosamine

demethoxycurcumin 60 μM treated group with the control group (Table 1). In the comparison of the *C. longa* extract treated group with the control group, the AUC value of alanine, arginine, aspartate, betaine, creatine, glutamate, glutathione, glycine, lactate, phenylalanine, threonine, uracil, and valine was 1.00, which makes it an excellent prediction biomarker. In general, AUC values of 0.9–1.0, 0.8–0.9, and 0.7–0.8 are considered excellent,

good, and fair predictive biomarkers, respectively [27]. In the comparison of the demethoxycurcumin 60 μM treated group with the control group, the AUC value of AMP, formate, glycine, lactate, NAD+, succinate, UDP-N-acetylglucosamine, UMP, uracil, uridine, myo-inositol, and glycerophosphocholine was also 1.00. The metabolites that showed the same change trend of concentration in the two comparisons with AUC over 0.7 were filtered. The result showed that lactate and uracil were increased after treatment with *C. longa* extract and demethoxycurcumin 60 μM, and aspartate, ATP, betaine, dimethylamine, formate, glycerophosphocholine, myo-inositol, and uridine were decreased after both treatments.

NMR spectra were binned for multivariate statistical analysis. On the PCA score plot of the *C. longa* extract treatment comparison, three groups were clearly separated (Fig. 3A). OPLS-DA was performed to confirm the difference between the control group and the *C. longa* extract treated group. The OPLS-DA score plot shows a clear separation between the two groups (Fig. 3B), and the S-line plot shows that metabolites contributed to this separation (Fig. 3C). Demethoxycurcumin treated groups were similarly classified on PCA and OPLS-DA score plots (Fig. 3D, E). The group with low-dose demethoxycurcumin treatment showed less difference from the control group, but the groups treated with 40 and 60 μM were similar and distributed far from the control group. As shown in the biomarker analysis, increased lactate and decreased uridine, myo-inositol, and dimethylamine were confirmed on the S-line plot of the comparison between control and demethoxycurcumin treated groups (Fig. 3F).

By comprehensively interpreting the results of multivariate statistical analysis and biomarker analysis, it was possible to identify significantly changed metabolites. Glutathione was upregulated and glutamate, which is involved in the biosynthesis of glutathione, was reduced by exposure to *C. longa* extract. Therefore, glutathione and glutamate had a negative correlation. It was reported that the α, β-unsaturated carbonyl group, which is contained in curcumin and curcumin derivatives, causes oxidative stress [28]. It was also reported that oxidative phosphorylation is reduced to lower the generation of reactive oxygen species as a mechanism to protect DNA and protein from oxidative stress [29]. This can increase lactate by increasing energy production using glycolysis. Pyruvate is converted to lactate by lactate dehydrogenase, with oxidation of NADH to NAD+. In the results of our study, a significant increase in lactate and an increase in NAD+ were confirmed (Fig. 4A). In addition, alanine, which is converted from pyruvate and glutamate by aminotransferase, was significantly increased and glutamate was decreased (Fig. 4B). An increase in
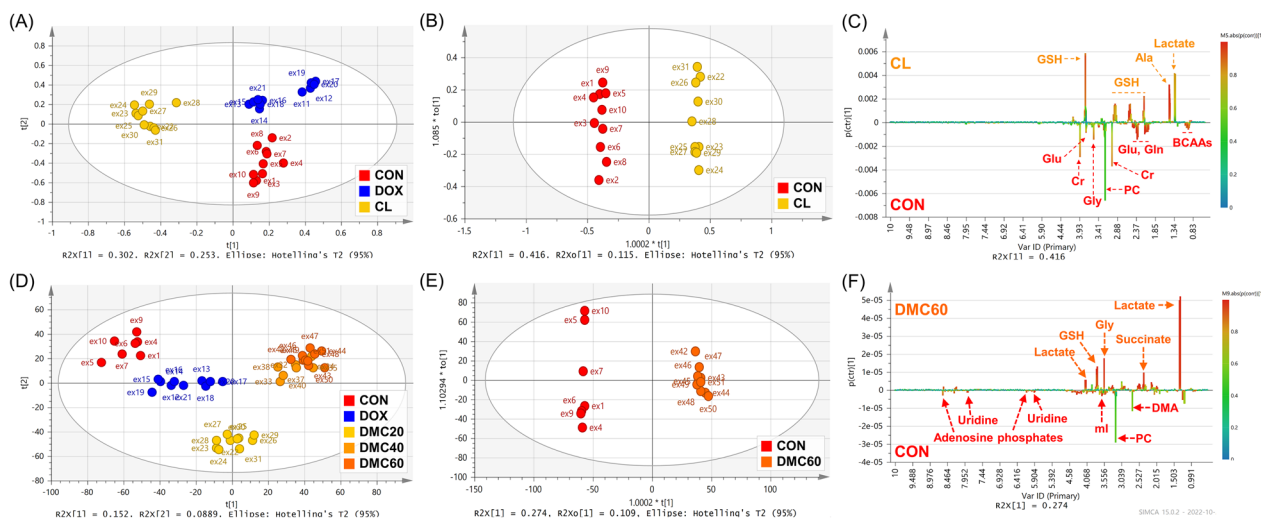
Fig. 3 Multivariate statistical analyses of NMR data. **A** PCA score plot of control group, doxorubicin treatment group and *C. longa* extract treatment group ($R^2X = 0.875$, $Q^2 = 0.722$), **B** OPLS-DA score plot of control group and *C. longa* extract treatment group ($R^2X = 0.531$, $R^2Y = 0.995$, $Q^2 = 0.983$), **C** OPLS-DA S-line plot of control group and *C. longa* extract treatment group, **D** PCA score plot of control group, doxorubicin treatment group and demethoxycurcumin treatment (20, 40, 60 μM) groups ($R^2X = 0.241$, $Q^2 = 0.15$), **E** OPLS-DA score plot of control group and demethoxycurcumin 60 μM treatment group ($R^2X = 0.383$, $R^2Y = 0.997$, $Q^2 = 0.928$), **F** OPLS-DA S-line plot of control group and demethoxycurcumin 60 μM treatment group
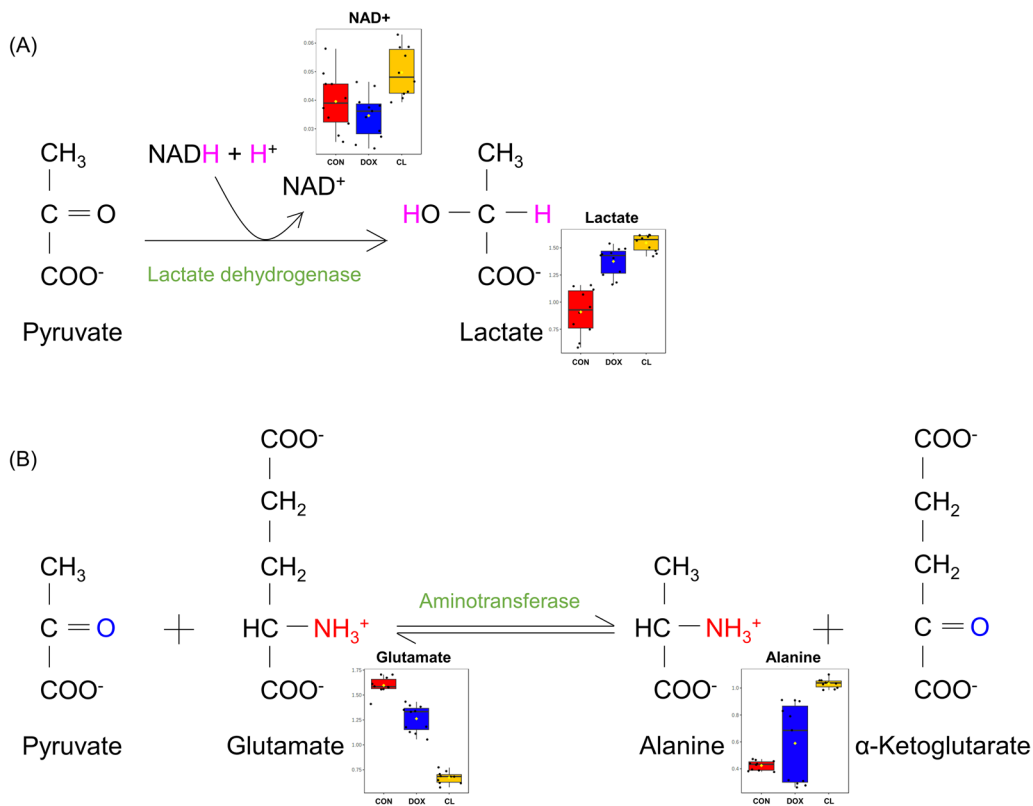
Fig. 4 Metabolic pathways involving significantly altered metabolites. **A** Pyruvate to lactate reduction by lactate dehydrogenase, **B** Cahill cycle by aminotransferase

energy production using glycolysis may result from mitochondrial damage. In a previous report, boiled extract of *C. longa* induced apoptosis by reducing the membrane potential through mitochondrial damage in glioma (A172), prostate cancer (PC3), and uterine cancer (HeLa) cell lines [3]. *C. longa* extract, which is a mixture of various compounds, can inhibit cancer cells through various mechanisms. The root of *C. longa* contains approximately 2% curcumin [30], and much research has been done on the activity of curcumin. The root of *C. longa* also contains curcumin derivatives, among which demethoxycurcumin accounts for roughly one-third of the curcumin content [31], and the activity of demethoxycurcumin on cancer cells has rarely been studied.

To confirm the inhibitory effect of demethoxycurcumin on cancer cells, we investigated the apoptosis-related proteins in HCT116 cells following demethoxycurcumin treatment by Western blot analysis. The expression levels of apoptosis-related proteins were evaluated by assessing pro-PARP, PARP, Bax, Bcl-2, and p53 protein levels in HCT116 cells incubated with normal medium (negative control), doxorubicin (positive control), or demethoxycurcumin (20, 40, and 60 μM) (Fig. 5). The β-actin content was confirmed to be constant, indicating that changes in these proteins cannot be explained by unequal loading of proteins. Demethoxycurcumin treatment at 40 and 60 μM significantly increased PARP, caspse-3, and caspase-9 cleavage. The increase in cleaved PARP was associated with a decrease in pro-PARP. Bax was upregulated following demethoxycurcumin treatment at 40 and 60 μM, whereas Bcl-2 was suppressed. Bax is

a pro-apoptotic protein belonging to the Bcl-2 family that moves to the mitochondrial outer membrane and oligomerizes to release cytochrome c into the cytoplasm [7]. Bax was increased by demethoxycurcumin treatment, whereas Bcl-2 expression was decreased. Cytochrome c released from the mitochondria served as an apoptosis signal and increased PARP, caspase-3, and caspase-9 cleavage according to demethoxycurcumin treatment. The expression of p53 was also increased with demethoxycurcumin treatment, and a greater increase with doxorubicin treatment was confirmed. Doxorubicin directly causes DNA damage in cancer cells and activates p53, which can cause apoptosis through activation of Bax. In this result, the doxorubicin treated group showed a significant increase in p53 compared to the demethoxycurcumin treated groups.

In the case of doxorubicin treatment, the PCA score plot of the metabolic data shows a significantly different distribution pattern from those of the *C. longa* extract and demethoxycurcumin treatment groups. This pattern can also be confirmed in the heatmap (Fig. 6). In particular, the amino acids tyrosine, methionine, isoleucine, leucine, arginine, phenylalanine, and valine showed a pattern of decreasing with doxorubicin treatment. This pattern was the same even with a low concentration of demethoxycurcumin, and the expression of apoptosis-related proteins in this group was similar to that of the control group. Therefore, it is considered that the decrease of these amino acids is not directly related to apoptosis. On the other hand, the decrease in 4-hydroxyproline, choline, NAD+, and glycerophosphocholine
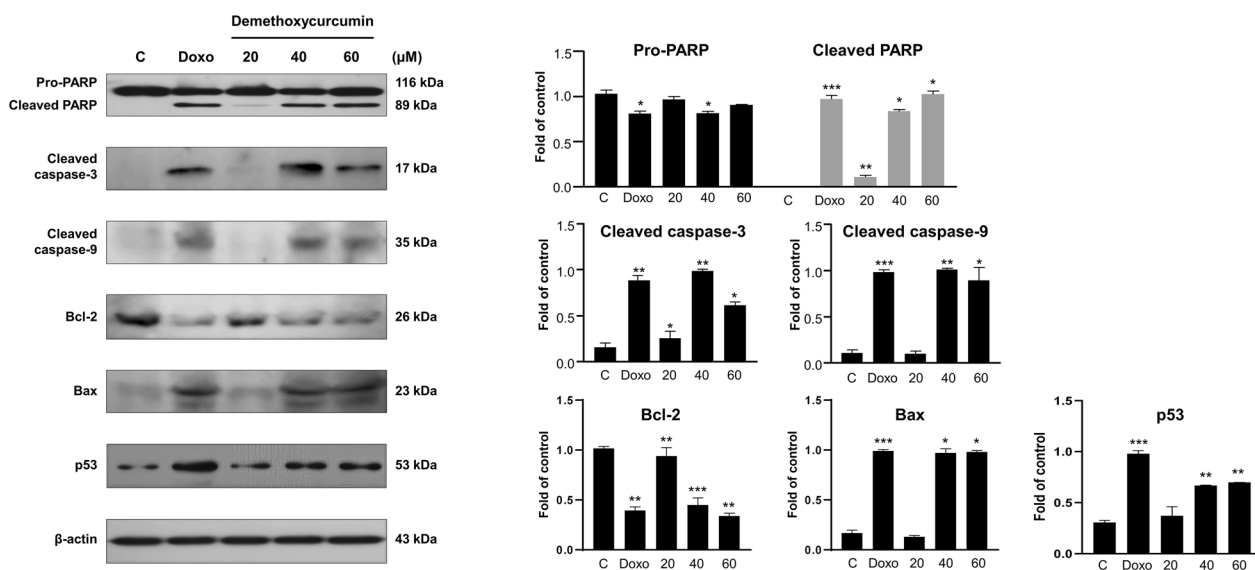

Fig. 5 Effects of demethoxycurcumin on apoptosis-related protein expression in HCT116 cells by western blot analysis. Data are presented as mean ± SD of three independent experiments (*$p < 0.05$, **$p < 0.01$, ***$p < 0.001$ versus control group)
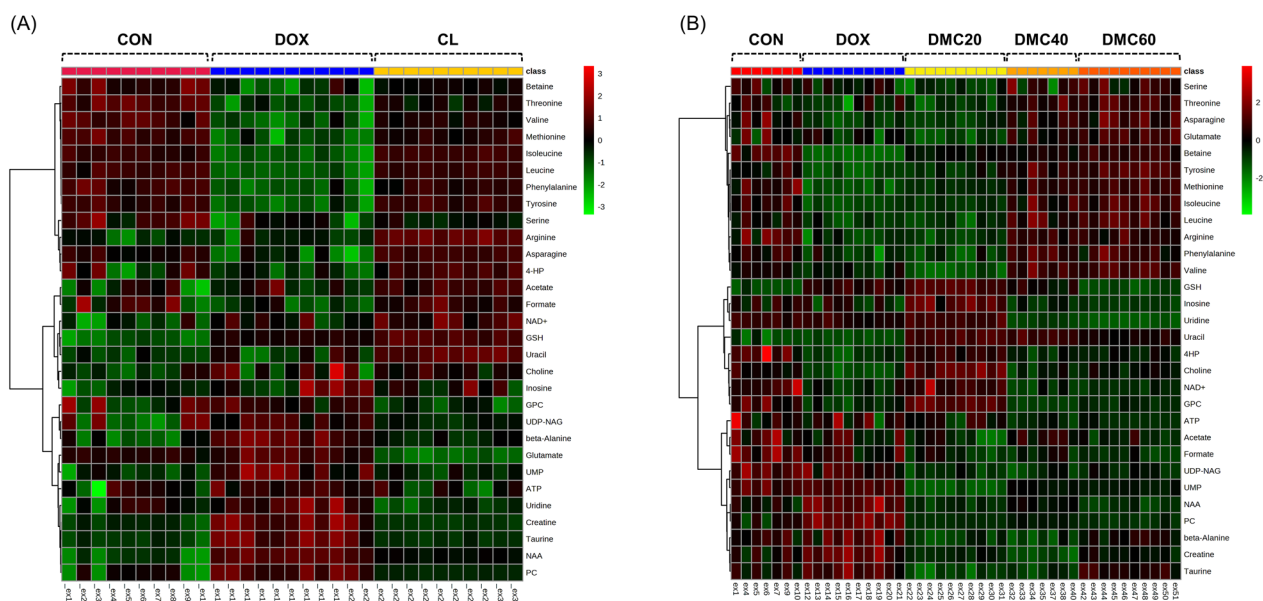
Fig. 6 Pearson correlation heatmap of metabolites in the HCT116 cell extracts. **A** Comparison of control group, doxorubicin treatment group and *C. longa* extract treatment group, **B** comparison of control group, doxorubicin treatment group and demethoxycurcumin treatment (20, 40, 60 μM) groups

in the doxorubicin and demethoxycurcumin (40 and 60 μM) groups was confirmed on the heatmap. Among them, choline and glycerophoshophcholine are part of the CDP-choline pathway, which is activated in cancer, and it was reported that glycerophosphocholine levels are characteristically high in cancer [32]. It was also

reported that cancer cells increase the uptake of choline and the biosynthesis of phosphatidylcholine, and, through their degradation, produce lipid mediators, such as free fatty acids used as fuel for β-oxidation, or phosphatidic acids for migration of cancer cells for escaping from immune cells. Phosphatidylcholine is the major
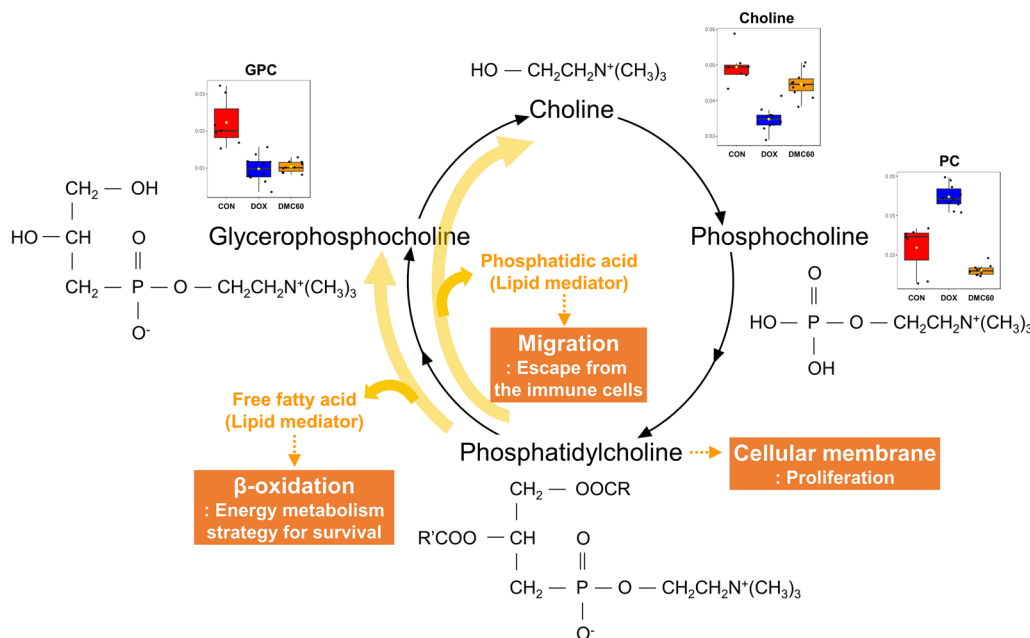

Fig. 7 CDP-choline pathway actively occurring for the survival of cancer cells

Yoon *et al. Applied Biological Chemistry*   (2023) 66:84

Page 9 of 10

component of the cellular membrane; therefore, its biosynthesis is closely related to the proliferation of cancer cells [33]. In our results, the contents of choline and glycerophosphocholine formed by the degradation of phosphatidylcholine were the highest in the control group, and were decreased with doxorubicin and demethoxycurcumin treatment. Phosphocholine, which is also part of the CDP-choline pathway, was decreased after treatment with demethoxycurcumin. It is considered that the CDP-choline pathway, which is activated for the survival of cancer cells, is blocked by treatment with demethoxycurcumin (Fig. 7).

Abbreviations

AUC	Area under the curve
NMR	Nuclear magnetic resonance
NOESY	Nuclear overhauser effect spectroscopy
PCA	Principal component analysis
OPLS-DA	Orthogonal partial least square discriminant analysis
RMSEE	Root mean square error
COSY	^{1}H-^{1}H correlation spectroscopy
HSQC	^{1}H-^{13}C heteronuclear single quantum coherence spectroscopy
ROC	Receiver operatic characteristic
TSP	3-(Trimethylsilyl) propionic acid-2,2,3,3

Supplementary Information

The online version contains supplementary material available at https://doi.org/10.1186/s13765-023-00844-9.

Additional file 1: Figure S1. Representative 2D ^{1}H-^{1}H COSY spectrum of HCT116 cell extract with metabolite annotation. **Figure S2**. Representative 2D ^{1}H-^{13}C HSQC-DEPT spectrum of HCT116 cell extract with metabolite annotation. **Table S1.** The list of identified metabolites in the HCT116 cell extract using NMR spectroscopy.

Author contributions
DYL managed the research project and editing the original manuscript. DY analyzed the data and wrote the paper. B-RC, W-CS, and K-WK performed formal analysis, Y-SL contributed to the plant material preparation. All authors read and approved the final manuscript.

Availability of data and materials
The datasets used and/or analysed during the current study are available from the corresponding author on reasonable request.

Declarations

Competing interests
The authors declare that they have no competing interests.

References

1. Prager GW, Braga S, Bystricky B, Qvortrup C, Criscitiello C, Esin E, Sonke GS, Martínez G, Frenel JS, Karamouzis M, Strijbos M, Yazici O, Bossi P, Banerjee S, Troiani T, Eniu A, Ciardiello F, Tabernero J, Zielinski CC, Casali PG, Cardoso F, Douillard JY, Jezdic S, McGregor K, Bricalli G, Vyas M, Ilbawi A (2018) Global cancer control: responding to the growing burden, rising costs and inequalities in access. ESMO Open 3(2):e000285
2. Cheng E, Blackburn HN, Ng K, Spiegelman D, Irwin ML, Ma X, Gross CP, Tabung FK, Giovannucci EL, Kunz PL, Llor X, Billingsley K, Meyerhardt JA, Fuchs CS (2021) Analysis of survival among adults with early-onset colorectal cancer in the national cancer database. JAMA Netw Open 4(6):e2112539–e2112539
3. Yoon J, Ryu B, Kim J, Yoon S (2006) Effects of Curcuma longa L. on some kinds of cancer cells. J Int Korean Med 27(2):429–443
4. Grover M, Behl T, Sehgal A, Singh S, Sharma N, Virmani T, Rachamalla M, Farasani A, Chigurupati S, Alsubayiel AM, Felemban SG, Sanduja M, Bungau S (2021) In vitro phytochemical screening, cytotoxicity studies of curcuma longa extracts with isolation and characterisation of their isolated compounds. Molecules 26(24):7509
5. Poompavai S, Gowri Sree V (2022) Anti-proliferative efficiency of pulsed electric field treated curcuma longa (Turmeric) extracts on breast cancer cell lines. IETE J Res 68(6):4555–4569
6. Ahmad R, Srivastava AN, Khan MA (2016) Evaluation of in vitro anticancer activity of rhizome of Curcuma longa against human breast cancer and Vero cell lines. Evaluation 1(1):1–6
7. Chen YC, Chen BH (2018) Preparation of curcuminoid microemulsions from Curcuma longa L. to enhance inhibition effects on growth of colon cancer cells HT-29. RSC Adv 8(5):2323–2337
8. Taebi R, Mirzaiey MR, Mahmoodi M, Khoshdel A, Fahmidehkar MA, Mohammad-Sadeghipour M, Hajizadeh MR (2020) The effect of Curcuma longa extract and its active component (curcumin) on gene expression profiles of lipid metabolism pathway in liver cancer cell line (HepG2). Gene Rep 18:100581
9. Kim J, Ha HL, Moon HB, Lee YW, Cho CK, Yoo HS, Yu DY (2011) Chemopreventive effect of Curcuma longa Linn on liver pathology in HBx transgenic mice. Integr Cancer Ther 10(2):168–177
10. Makaremi S, Ganji A, Ghazavi A, Mosayebi G (2021) Inhibition of tumor growth in CT-26 colorectal cancer-bearing mice with alcoholic extracts of Curcuma longa and Rosmarinus officinalis. Gene Rep 22:101006
11. Yang DS, Yang SJ (2013) Effects of curcuma longa L. on MDA-MB-231 human breast cancer cells and DMBA-induced breast cancer in rats. J Korean Obstet Gynecol 26(3):44–58
12. Lu JJ, Cai YJ, Ding J (2011) Curcumin induces DNA damage and caffeine-insensitive cell cycle arrest in colorectal carcinoma HCT116 cells. Mol Cell Biochem 354(1):247–252
13. Kim KC, Lee C (2010) Curcumin induces downregulation of E2F4 expression and apoptotic cell death in HCT116 human colon cancer cells; involvement of reactive oxygen species. Korean J Physiol Pharma 14(6):391–397
14. Collett GP, Campbell FC (2004) Curcumin induces c-jun N-terminal kinase-dependent apoptosis in HCT116 human colon cancer cells. Carcinogenesis 25(11):2183–2189
15. Tamvakopoulos C, Dimas K, Sofianos ZD, Hatziantoniou S, Han Z, Liu ZL, Wyche JH, Pantazis P (2007) Metabolism and anticancer activity of the curcumin analogue, dimethoxycurcumin. Clin Cancer Res 13(4):1269–1277
16. Yodkeeree S, Chaiwangyen W, Garbisa S, Limtrakul P (2009) Curcumin, demethoxycurcumin and bisdemethoxycurcumin differentially inhibit cancer cell invasion through the down-regulation of MMPs and uPA. J Nutr Biochem 20(2):87–95
17. Yodkeeree S, Ampasavate C, Sung B, Aggarwal BB, Limtrakul P (2010) Demethoxycurcumin suppresses migration and invasion of MDA-MB-231 human breast cancer cell line. Eur J Pharmacol 627(1–3):8–15

18. Ni X, Zhang A, Zhao Z, Shen Y, Wang S (2012) Demethoxycurcumin inhibits cell proliferation, migration and invasion in prostate cancer cells. Oncol Rep 28(1):85–90
19. Liu YL, Yang HP, Gong L, Tang CL, Wang HJ (2011) Hypomethylation effects of curcumin, demethoxycurcumin and bisdemethoxycurcumin on WIF-1 promoter in non-small cell lung cancer cell lines. Mol Med Rep 4(4):675–679
20. Ko YC, Lien JC, Liu HC, Hsu SC, Lin HY, Chueh FS, Ji BC, Yang MD, Hsu WH, Chung JG (2015) Demethoxycurcumin-induced DNA damage decreases DNA repair-associated protein expression levels in NCI-H460 human lung cancer cells. Anticancer Res 35(5):2691–2698
21. Chen Y, Wu M (2021) Demethoxycurcumin inhibits the growth of human lung cancer cells by targeting of PI3K/AKT/m-TOR signalling pathway, induction of apoptosis and inhibition of cell migration and invasion. Trop J Pharm Res 20(4):687–693
22. Kao CC, Cheng YC, Yang MH, Cha TL, Sun GH, Ho CT, Lin YC, Wang HK, Wu ST, Way TD (2021) Demethoxycurcumin induces apoptosis in HER2 overexpressing bladder cancer cells through degradation of HER2 and inhibiting the PI3K/Akt pathway. Environ Toxicol 36(11):2186–2195
23. Lin CC, Kuo CL, Huang YP, Chen CY, Hsu MJ, Chu YL, Chueh FS, Chung JG (2018) demethoxycurcumin suppresses migration and invasion of human cervical cancer HeLa cells via inhibition of NF-κB pathways. Anticancer Res 38(5):2761–2769
24. Chien MH, Yang WE, Yang YC, Ku CC, Lee WJ, Tsai MY, Lin CW, Yang SF (2020) Dual targeting of the p38 mapk-ho-1 axis and ciap1/xiap by demethoxycurcumin triggers caspase-mediated apoptotic cell death in oral squamous cell carcinoma cells. Cancers 12(3):703
25. Huang C, Lu HF, Chen YH, Chen JC, Chou WH, Huang HC (2020) Curcumin, demethoxycurcumin, and bisdemethoxycurcumin induced caspase-dependent and–independent apoptosis via Smad or Akt signaling pathways in HOS cells. BMC Complement Med Ther 20(1):1–11
26. Su RY, Hsueh SC, Chen CY, Hsu MJ, Lu HF, Peng SF, Chen PY, Lien JC, Chen YL, Chueh FS, Chung JG, Yeh MY, Huang YP (2021) Demethoxycurcumin suppresses proliferation, migration, and invasion of human brain glioblastoma multiforme GBM 8401 cells via PI3K/Akt pathway. Anticancer Res 41(4):1859–1870
27. Xia J, Broadhurst DI, Wilson M, Wishart DS (2013) Translational biomarker discovery in clinical metabolomics: an introductory tutorial. Metabolomics 9(2):280–299
28. Niki E (2009) Lipid peroxidation: physiological levels and dual biological effects. Free Radic Biol Med 47(5):469–484
29. Brand KA, Hermfisse U (1997) Aerobic glycolysis by proliferating cells: a protective strategy against reactive oxygen species 1. Faseb J 11(5):388–395
30. Anderson AM, Mitchell MS, Mohan RS (2000) Isolation of curcumin from turmeric. J Chem Educ 77(3):359
31. Lee YS, Oh SM, Li QQ, Kim KW, Yoon D, Lee MH, Kwon DY, Kang OH, Lee DY (2022) Validation of a quantification method for curcumin derivatives and their hepatoprotective effects on nonalcoholic fatty liver disease. Curr Issues Mol Biol 44(1):409–432
32. Sonkar K, Ayyappan V, Tressler CM, Adelaja O, Cai R, Cheng M, Glunde K (2019) Focus on the glycerophosphocholine pathway in choline phospholipid metabolism of cancer. NMR in Biomed 32(10):e4112
33. Saito RDF, Andrade LNDS, Bustos SO, Chammas R (2022) Phosphatidylcholine-derived lipid mediators: the crosstalk between cancer cells and immune cells. Front Immunol 13:215

Publisher's Note